

Synthesis and microwave absorbing property of the dendritic $Fe_{0.6}Co_{0.4}$ alloy

LIANGLIANG TIAN^{*}, FEI WANG^a

Department of Research center for materials interdisciplinary science, Chongqing University of arts and sciences, Chongqing, PR China

^aInstitute of Modern Physics, Chinese Academy of Sciences, Lanzhou, PR China

Dendritic $Fe_{0.6}Co_{0.4}$ alloy was synthesized by low temperature hydrothermal method under strong alkaline condition. Morphology, composition, structure, magnetic property and microwave absorbing property of the $Fe_{0.6}Co_{0.4}$ alloy were characterized by scanning electron microscopy (SEM), energy diffraction spectrum (EDS), X-ray diffraction (XRD), vibrating sample magnetometer (VSM) and vector network analyzer, respectively. XRD pattern reveals that the alloy shows bcc structure. The saturation magnetization, coercivity and residual magnetization is 212.39 emu/g, 56.0 Oe and 9.1 emu/g, respectively. The microwave absorbing property demonstrates that the minimum RL of the $Fe_{0.6}Co_{0.4}$ alloy is -14.08 dB at 3.1 GHz with a thickness 6.5 mm.

(Received November 20, 2012; accepted September 18, 2013)

Keywords: Dendritic, FeCo alloy, Microwave absorbing property, Permittivity, Permeability

1. Introduction

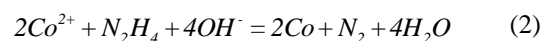
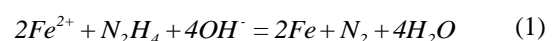
With the development of electronic technology, electromagnetic interference pollution has become a problem due to the wide application of electromagnetic systems, radar system [1-2]. In order to solve the problem, microwave absorption materials have attracted lots of attention in recent years. Lots of materials were prepared as microwave absorption materials, such as ferrite [3], CuO [4], etc. It is known that magnetic metals (Fe, Co and Ni) and their composites possess excellent microwave absorbing property because of the strong attenuation caused by dielectric loss and magnetic loss [5, 6]. Y. Feng reported Fe-50wt%Ni alloy as microwave absorbing material. It is found that morphology of the FeNi alloy changed from spherical to flaky with the increase of the milling time. Simultaneously, the microwave absorbing property was enhanced with the change of the morphology [7]. Fe_3Co_2 nanocrystal powders were synthesized by mechanical alloying and it is reported that the microwave property of the alloy depended on structure and morphology of the particles [8]. On the basis of above reports, the microwave absorbing property can be strongly influenced by the morphology.

In this article, dendritic $Fe_{0.6}Co_{0.4}$ alloy was synthesized by low temperature hydrothermal method. Microwave absorbing property of the $Fe_{0.6}Co_{0.4}$ alloy was tested in the range of 0-8 GHz. It is revealed that the dendritic $Fe_{0.6}Co_{0.4}$ alloy shows excellent microwave absorbing property in the range of 0-8 GHz. This kind of

FeCo alloy has potential applications in the field of microwave absorption.

2. Experiment

In this experiment, all chemicals are of analytical grade and used without further purification. In a typical experiment, $FeSO_4 \cdot 7H_2O$ (6 ml. 0.1 M) and $CoCl_2 \cdot 6H_2O$ (4ml, 0.1M) were dissolved in 4 ml cetyltrimethylammonium bromide (CTAB) aqueous solution (0.1 M). Then 10 ml sodium hydroxide (NaOH) solution (25 M) and 4ml hydrazine hydrate ($NH_2-NH_2 \cdot H_2O$)(85 wt.%) were added. The final solution was stirred homogeneously and transferred into a 50 ml reaction kettle. After that, the reactor was put into a drying oven at 130°C and aged at 200°C for 2h. The reactor was cooled down to room temperature in the air. The products were collected and washed for several times and finally dried for 12 hours in an oven at 60°C. The reduction process of Fe^{2+} and Co^{2+} can be expressed as follows:



In order to measure the microwave property, 10 vol% $Fe_{0.6}Co_{0.4}$ /paraffin composite sample was prepared by uniformly mixing the $Fe_{0.6}Co_{0.4}$ alloy and paraffin matrix. The composite was compacted into ring shape with 7.00

mm outer diameter and 3.04 mm inner diameter. The reflection loss (*RL*) of a microwave absorption material can be calculated by the following equations:

$$R = 20 \log \left| \frac{Z_I - Z_0}{Z_I + Z_0} \right| \quad (3)$$

$$Z_I = \sqrt{\frac{\mu_0 \mu}{\epsilon_0 \epsilon}} \tanh(j2\pi f d \sqrt{\mu_0 \mu \epsilon_0 \epsilon}) \quad (4)$$

Where Z_I is the input impedance, Z_0 is the free space impedance; d is the thickness of the absorber. c and f is the light velocity and the frequency of microwave, respectively. ϵ_0 and μ_0 is vacuum permittivity and vacuum permeability, respectively. ϵ and μ is complex permittivity and complex permeability, respectively.

The morphology and chemical composition of the Fe_{0.6}Co_{0.4} alloy was analyzed on a Hitachi S-4800 field emission scanning electron microscope (FESEM). X-ray diffraction (XRD) measurement was performed on a Rigaku D/Max-2400 X-ray diffractometer using Cu K α radiation (40 kV, 60 mA). Static magnetic property was characterized by vibrating sample magnetometer (VSM) (Lak Shore 7304). High frequency electromagnetic property was measured using a vector network analyzer (VNA).

3. Results and discussion

3.1 Structure and morphology of the Fe_{0.6}Co_{0.4}

EDS pattern of the Fe_{0.6}Co_{0.4} alloy was shown in Fig. 1a. The content of Fe and Co is 58.39 atom% and 41.61 atom% in the alloy, respectively. Note that the composition of the Fe_{0.6}Co_{0.4} alloy is consistent with the mole ratio of Fe²⁺ and Co²⁺ in the solution, indicating the complete reduction of Fe²⁺ and Co²⁺. The result is different from the FeCo alloys synthesized by electrodeposition. In our previous research, it is found that the Fe content in the alloys is always higher than that in solution due to the anomalous codeposition [9]. Fig. 1b displays the XRD pattern of the obtained Fe_{0.6}Co_{0.4} alloy. As can be seen from Fig. 1b, Fe_{0.6}Co_{0.4} alloy shows only bcc structure. The peaks located at 44.9°, 65.4°, 82.7° and 99.5° are clearly found in the pattern, corresponding to (110) (200) (211) and (220) diffraction peaks, respectively. In addition, bcc (110) displays stronger preferred orientation than the other peaks. Morphology of the Fe_{0.6}Co_{0.4} alloy was investigated by SEM and shown in Fig. 1c. It is evident that Fe_{0.6}Co_{0.4} alloy shows branch morphology and two lines of leaves grow along the branch. As we can see from the inset of Fig. 1c, the size of the leaves is not uniform and the leaves are about 2-3 μ m long and 1-2 μ m wide.

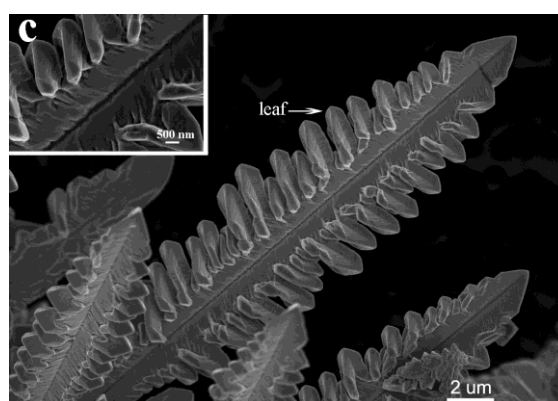
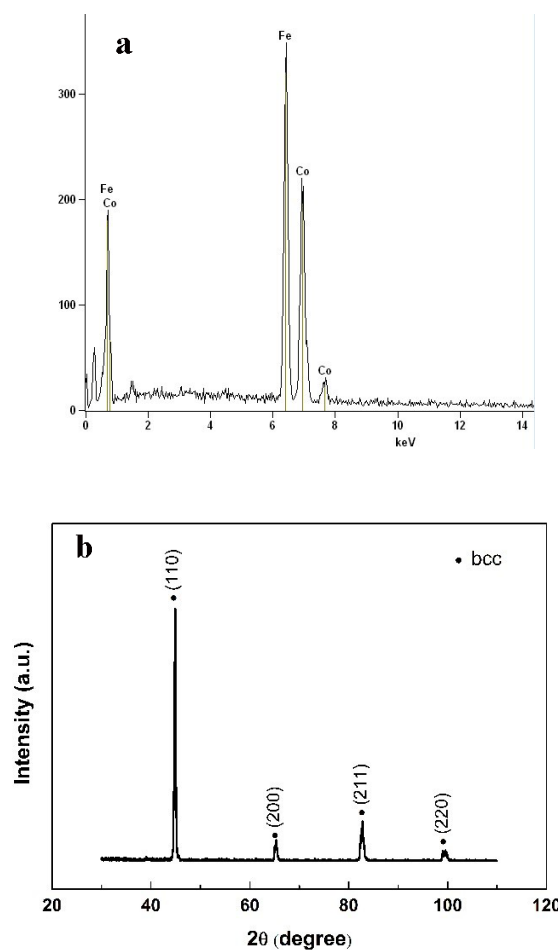


Fig. 1. EDS pattern (a) and XRD pattern (b) of the Fe_{0.6}Co_{0.4} alloy. (c) is the SEM image of the Fe_{0.6}Co_{0.4} alloy. Inset of (c) is the image with high magnification.

3.3 Magnetic property of the Fe_{0.6}Co_{0.4} alloy

Magnetic property of the Fe_{0.6}Co_{0.4} alloy was measured by VSM and displayed in Fig. 2. It is clear that the Fe_{0.6}Co_{0.4} alloy possesses high M_s and low H_c . The saturation magnetization (M_s) and coercivity (H_c) of the Fe_{0.6}Co_{0.4} alloy is about 212.39 emu/g and 56.0 Oe,

respectively. The residual magnetization is about 9.1 emu/g. It is known that the magnetic moment of Fe ($2.2 \mu_B$) is larger than that of Co ($1.7 \mu_B$), indicating that the M_s of Fe is higher than that of Co. However, the magnetic anisotropic constant of Co (2.7×10^6 erg/cm³) is much larger than that of Fe (4.81×10^5 erg/cm³), indicating that the H_c of Co is much higher than that of Fe. In the $Fe_{0.6}Co_{0.4}$ alloy, Fe content is higher than Co. Therefore, the $Fe_{0.6}Co_{0.4}$ alloy displays higher magnetization and lower coercivity.

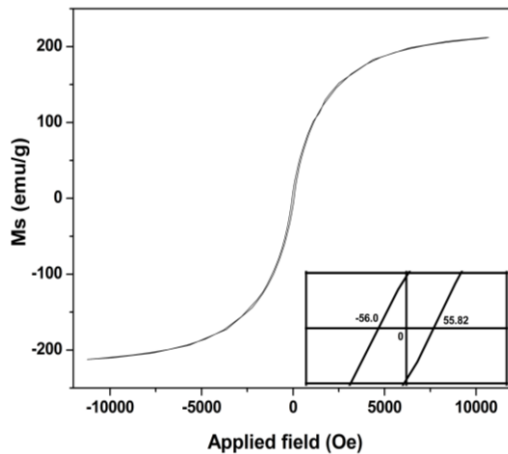


Fig. 2. Magnetic hysteresis loop of the $Fe_{0.6}Co_{0.4}$ alloy.

3.4 Microwave absorbing property of the $Fe_{0.6}Co_{0.4}$ alloy

Generally speaking, microwave absorption mechanism of the absorption materials can be concluded into dielectric loss and magnetic loss. In order to investigate the intrinsic reasons for microwave absorption property, the permittivity and permeability of the $Fe_{0.6}Co_{0.4}$ alloy were measured. Fig. 3a shows the complex permittivity, it is indicated that the value of ϵ' is between 7.8 and 10 and ϵ' decreases with the increase of the frequency. In addition, there is a wide peak at about 3.8 GHz. ϵ'' value is between 0.5 and 1.3 and there is a wide peak at about 5.0 GHz. Fig. 3b displays the complex permeability of the $Fe_{0.6}Co_{0.4}$ alloy. It is evident that the value of μ' is between 1.2 and 3.5 and μ' decreases with the increase of the frequency. The value of μ'' is between 0.15 and 0.7. Moreover, there is a peak located at 1.4 GHz and the peak can be attributed to the consistent natural resonance peak.

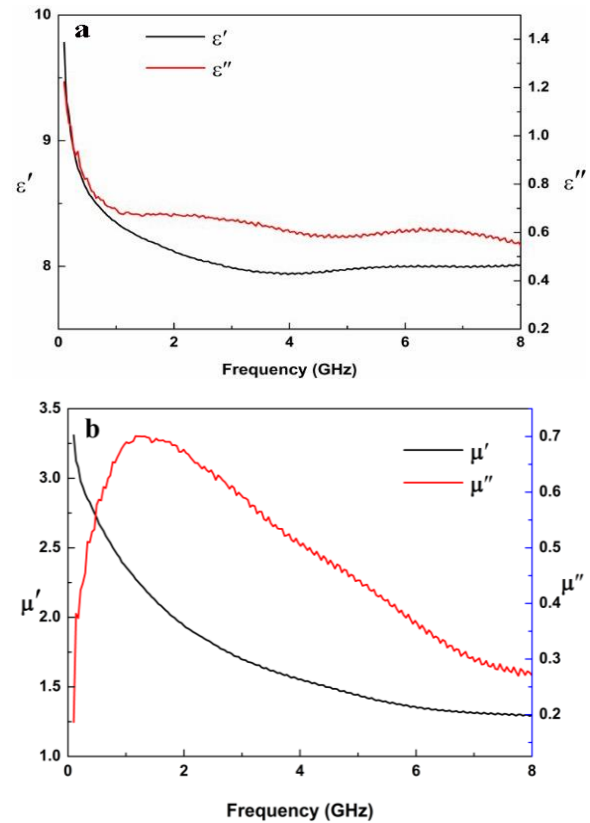


Fig. 3. The complex permittivity and complex permeability of the $Fe_{0.6}Co_{0.4}$ alloy. (a) ϵ' and ϵ'' . (b) μ' and μ'' .

Microwave absorbing property of the $Fe_{0.6}Co_{0.4}$ alloy within 0-8 GHz was measured and pictured in Fig. 4. According to Eq. (3) and (4), when the RL is -10 dB the attenuation of microwave achieves 90%. As can be seen from Fig. 4, the reflectivity of $Fe_{0.6}Co_{0.4}$ is smaller than -10 dB with all the thickness in the range of 2.3-8.0 GHz. Moreover, with the thickness increase, the reflectivity first decreases, showing a minimum value -14.08 dB, and then increases. In conclusion, the minimum RL of the $Fe_{0.6}Co_{0.4}$ alloy is -14.08 dB at 3.1 GHz with a thickness 6.5 mm. The dendritic $Fe_{0.6}Co_{0.4}$ alloy has potential applications in microwave absorption.

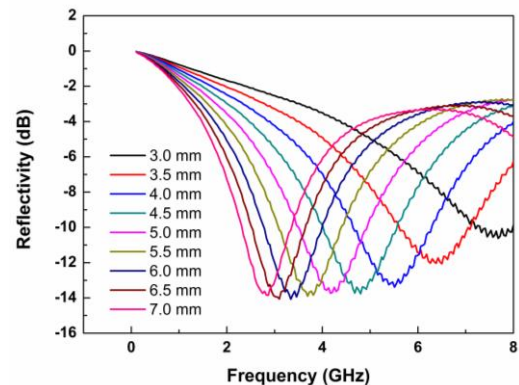


Fig. 4. Reflectivity curves of the $Fe_{0.6}Co_{0.4}$ alloy with different thickness.

4. Conclusions

Dendritic $Fe_{0.6}Co_{0.4}$ alloy was successfully synthesized by low temperature hydrothermal method. XRD pattern reveals that the $Fe_{0.6}Co_{0.4}$ alloy shows only bcc structure. The saturation magnetization (M_s), coercivity (H_c) and residual magnetization is 212.39 emu/g, 56.0 Oe and 9.1 emu/g, respectively. The microwave absorbing result demonstrates that the minimum RL of the $Fe_{0.6}Co_{0.4}$ alloy is -14.08 dB at 3.1 GHz with a thickness 6.5 mm.

Reference

- [1] I. Cuinas, Electronics. Lett **41**, 340 (2005).
- [2] A. Balmori, Pathophysiol **16**, 191 (2009).
- [3] J. H. Kim, S. S. Kim, J. Alloys Compd **509**, 4399 (2011).
- [4] J. Zeng, J. C. Xu, P. Tao, W. Hua, J. Alloys Compd **487**, 304 (2009).
- [5] Y. Feng, T. Qiu, J. Alloys Compd **513**, 455 (2012).
- [6] K. Park, J. Han, S. Lee, J. Yi, Compos Part A-Appl S. **42**, 573 (2011).
- [7] Y. Feng, T. Qiu, J. Magn. Magn. Mater **324**, 2528 (2012).
- [8] P. Zhou, L. Deng, J. Xie, D. Liang, J. Alloys Compd **448**, 303 (2008).
- [9] C. Qiang, J. Xu, S. Xiao, Y. Jiao, Z. Zhang, Y. Liu, L. Tian, Z. Zhou, Appl. Surf. Sci **257**, 1371 (2010).

*Corresponding author: tianll07@163.com